Bioorganic & Medicinal Chemistry 18 (2010) 100–110

Contents lists available at ScienceDirect

Bioorganic & Medicinal Chemistry

journal homepage: www.elsevier.com/locate/bmc

Identification of a novel ligand binding motif in the transthyretin channel

Luis Mauricio T. R. Lima [a,*], Vivian de Almeida Silva [a,b,c], Leonardo de Castro Palmieri [a], Maria Clara B. R. Oliveira [a], Débora Foguel [c], Igor Polikarpov [d,*]

[a] Faculdade de Farmácia, Universidade Federal do Rio de Janeiro, RJ, 21941-902, Brazil
[b] Centro Federal de Educação Tecnológica em Química, RJ, Brazil
[c] Instituto de Bioquímica Médica, Universidade Federal do Rio de Janeiro, RJ 21941-902, Brazil
[d] Instituto de Física de São Carlos, Universidade de São Paulo, Avenida Trabalhador São Carlense, 400, CEP 13566-590 São Carlos, SP, Brazil

ARTICLE INFO

Article history:
Received 11 August 2009
Revised 5 November 2009
Accepted 6 November 2009
Available online 12 November 2009

Keywords:
Transthyretin
Amyloid
Hormone binding site
Naphthalenesulfonate

ABSTRACT

The design of therapeutic compounds targeting transthyretin (TTR) is challenging due to the low specificity of interaction in the hormone binding site. Such feature is highlighted by the interactions of TTR with diclofenac, a compound with high affinity for TTR, in two dissimilar modes, as evidenced by crystal structure of the complex. We report here structural analysis of the interactions of TTR with two small molecules, 1-amino-5-naphthalene sulfonate (1,5-AmNS) and 1-anilino-8-naphthalene sulfonate (1,8-ANS). Crystal structure of TTR:1,8-ANS complex reveals a peculiar interaction, through the stacking of the naphthalene ring between the side-chain of Lys15 and Leu17. The sulfonate moiety provides additional interaction with Lys15′ and a water-mediated hydrogen bond with Thr119′. The uniqueness of this mode of ligand recognition is corroborated by the crystal structure of TTR in complex with the weak analogue 1,5-AmNS, the binding of which is driven mainly by hydrophobic partition and one electrostatic interaction between the sulfonate group and the Lys15. The ligand binding motif unraveled by 1,8-ANS may open new possibilities to treat TTR amyloid diseases by the elucidation of novel candidates for a more specific pharmacophoric pattern.

1. Introduction

Transthyretin (TTR) form a β-sheet rich, homotetrameric 3D structure.[1,2] Under certain conditions, TTR can unfold and aggregate into amyloid fibrils, through a well characterized monomeric pathway.[3,4] This results in TTR amyloidosis diseases such as senile systemic amyloidosis (SSA), familial amyloid polyneuropathy (FAP), familial amyloid cardiomyopathy (FAC) and central nervous systems amyloidosis (CNSA).[5–7] To date, the only approved clinical approach for treatment of TTR-related diseases is liver transplantation to replace mutant TTR to wild-type tTTR (wtTTR),[8] which is not effective against wild-type TTR deposition in SSA. In this context, the search for other therapeutic alternatives is highly desirable.

TTR carries thyroxine (T4) in the blood, although it is not the main carrier in humans. The two binding sites, denominated hormone binding sites (HBS), are located on the twofold symmetry axis, at the interface between the two dimers that comprise the tetramer. The binding of ligands to TTR can increase TTR stability by decreasing the extent of tetramer dissociation and consequently amyloid aggregation and fibril formation.[9] These features make attractive the screening for potent ligands aiming to decrease TTR dissociation. However, a complicating factor in the design of specific ligands to TTR lies in the fact that TTR can effectively bind a large diversity of chemically unrelated compounds with moderate to high affinity. This low specificity is due to the wide, non-polar properties of the binding channels, limited electrostatic and hydrogen bonding groups. As a consequence, circulating compounds in the serum would act as competitive inhibitors, hence demanding a great effort in the optimization of specific and high-affinity TTR ligands.[10,11] Despite of these weakly restrictive properties of the TTR binding site, some non-physiological ligands can interact with TTR with very high affinity, with dissociation constants (K_d) reaching nanomolar range.[11–14]

Commercial drugs originally designed for treating other diseases have been screened for their ability to TTR binding and kinetic stabilization, some already covered by patents, and a few entered clinical trials (e.g., diflunisal;[15] USA Clinical Trials Identifiers: NCT00294671, NCT00409175). Most of these compounds have the advantage of being FDA approved drugs. However, their primary activities for which they were designed for, become side effects in TTR-related disease applications. In this context,

Abbreviations: 1,8-ANS, 1-anilino-8-naphthalene sulfonate, ammonium salt; 1,5-AmNS, 1-amino-5-naphthalene sulfonate, potassium salt; TTR, human transthyretin; T4, thyroxine.

* Corresponding authors. Address: Faculdade de Farmácia, Universidade Federal do Rio de Janeiro, CCS-Bss34, Rio de Janeiro, RJ 21941-590, Brazil. Tel./fax: +55 21 2562 6639 (L.M.T.R.L.); tel./fax: +55 16 3373 8088 (I.P.).
E-mail addresses: mauricio@pharma.ufrj.br (L.M.T.R. Lima), ipolikarpov@if.sc.usp.br (I. Polikarpov).

0968-0896/$ - see front matter © 2009 Published by Elsevier Ltd.
doi:10.1016/j.bmc.2009.11.025

structure-based optimization of lead compounds with better specificity for TTR would be required.

In this work, we report the crystal structure of TTR in complex with two aminonaphthalene sulfonate compounds. Both ligands (Fig. 1), 1-amino-5-naphthalene sulfonate (1,5AmNS) and 1-anilino-8-naphthalene sulfonate (1,8ANS) bind to the HBS. Remarkably, 1,8-ANS, a widely used fluorescent probe, displays novel features in the interaction with TTR. 1,8-ANS binds to an extension of the HBS sandwiching its naphthalene ring between the side-chains of Lys15 and Leu17, a position which has not yet been described. We discuss the possibility to explore this novel binding motif of the HBS revealed here by 1,8-ANS for the design of more specific TTR ligands with the potential of therapeutic applications.

2. Results

A contemporary approach in the pipeline of drug discovery is the *fragment-based screening*,[16–21] which allows both the identification of structural binding motifs in the target as well as low molecular weight compounds with moderate activity, ideal for further steps in optimization of desired drug-like properties.[22] The competitive ligand displacement is an attractive method in the process of high throughput screening. Such an approach has been used with TTR a few times, applying radioactive analogues in the characterization of xantones[13] and utilizing the fluorescent probe 1,8-ANS in the measurement of binding of T4 and other compounds.[23–26] The latter approach has advantages such as being non-radioactive, simple and inexpensive. Despite the extensive use of 1,8-ANS for a large number of applications, including binding to TTR,[23–25,27] the detailed mechanism of its interactions has been described for only a few protein structures in complex with 1,8-ANS.[28,29] 1,8-ANS interaction with TTR has been applied for both measurements of competitive ligand binding with T4 and access of a proper protein folding. Although it is usually well accepted that 1,8-ANS binds to the HBS[23–25] the precise molecular details of its binding with TTR is not available yet.

2.1. Evaluation of TTR interaction with 1,8-ANS and 1,5-AmNS

It has been reported that 1,8-ANS binding to wtTTR occurs in the micromolar concentration range[24] (Table 1). However, no data have been published regarding the binding affinity of 1,8-ANS to others TTR variants. We then decided to investigate the interaction of 1,8-ANS and 1,5-AmNS with two TTR variants with distinctive functional features, the V30M (aggressive[6]) and T119M (transsupressor[30]).

Initially, we determined the K_d for 1,8-ANS binding following the increase in its fluorescence intensity upon complexation with TTR (Fig. 2 and Table 1). Complex formation of 1,8-ANS with wtTTR, V30M and T119M occurs with similar affinity, with dissociation constants (K_d) of approximately 5 μM (using two interactive sites model and Hill '*n*' equal to unity; Table 1). We also calculated the K_d considering two independent binding models. However, although application of this model results in K_d similar to the previously reported binding assays, errors associated to fitting were too high to be sufficiently confident. From these analysis, we consider that the two binding sites are similar in affinity and that they can be more properly described, with better precision and accuracy, by the simpler, non-interactive, independent binding model, as suggested elsewhere.[23,25]

The 1,5-AmNS also binds to wtTTR as indicated by the progressive increase in fluorescence anisotropy of the compound (Fig. 3A) and by the quenching of protein intrinsic fluorescence (Fig. 3B). Measurement of K_d for 1,5-AmNS was accessed from the dependence of TTR intrinsic fluorescence intensity on ligand concentration (Fig. 3B), and the obtained constants are reported in Table 1. The binding of 1,5-AmNS to these three different TTR variants are similar in affinity as well, with K_d of approximately 80 μM (Table 1).

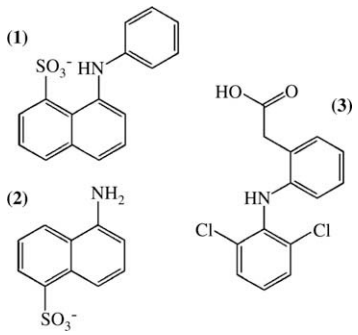

Figure 1. Chemical structure of 1,8-ANS (**1**), 1,5-AmNS (**2**) and diclofenac (**3**).

2.2. Crystal structure of apo wtTTR

No high resolution structural information of TTR in complex with the naphthalenesulfonate compounds is available to date. To better understand the molecular details of the interaction, we solved the crystal structures of wtTTR in the apo form and in complex with these two ligands, at exactly the same crystallization conditions.

The structure of wtTTR in the apo form was determined at 1.6 Å resolution and belongs to the orthorhombic space group $P2_12_12$, with a TTR dimer in the asymmetric unit (Table 2). The apo TTR structure was solved by molecular replacement using 1.5 Å resolution TTR structure (PDB id: 1F41) as a search model. Calculated electron density is well defined for the amino acids 10–125 in both monomers of the dimer. These monomers were refined independently (Fig. 4). Similar to previously reported apo wtTTR structures,[31] there are considerable changes in TTR conformation between these monomers, reported, for example, by significant Cα-RMSD between these two polypeptide chains. These alterations are mainly located in the BC loop (amino acids 38–40; up to 1.5 Å RMSD) and in the F–G loop (aminoacids 98–104; up to 6.5 Å RMSD). Deviations between monomers structures would arise both from intrinsic folding properties of the protein and from the orthorhombic crystal packing.

In comparison with the several apo structures reported to date, our apo wtTTR model displays similar cell unit parameters, space group and crystallographic contacts, differing by only 1 Å or less in the overall RMS deviations. These structures determined from the crystals grown in different crystallizations precipitants (PEG, PEG MME, ammonium sulfate) and pH (7.4–4.6) indicate a common, most probable and populated protein fold for TTR.

2.3. Overall effects of ligand binding

The wtTTR crystal structures with 1,8-ANS, 1,5-AmNS and diclofenac were obtained by soaking of the apo wtTTR crystals into the crystallization media containing saturating amounts of the respective compounds. For all crystals tested, a discrete decrease in resolution was observed as compared to the apo wtTTR, indicative of crystal rearrangements due to ligand binding (Table 2). The wtTTR:ligand structures were solved by molecular replacement using the apo wtTTR structure presented here as a search model. Again, amino acids 10–125 were well defined for both monomers (Fig. 4). Inspection of the HBS in these structures with 2 $|F_o| - |F_c|$ map contoured at 1σ and the difference map $|F_o| - |F_c|$ contoured at 3σ revealed the presence of bound

Table 1
Dissociation constants for TTR interaction with 1,8-ANS and 1,5-AmNS

Ligand	Independent model		Interactive model		Experimental	Ref.
	K_{d1} (μM)	K_{d2} (μM)	K_d (μM)	Hill '*n*'	description	
1,8 ANS	1.1	4.8	1.8	–	wt TTR[b]	23
	–	–	10	–	wt TTR[c]	25
	1.1[a]	4.8[a]	4.3 ± 0.6	1.0 ± 0.2	wt TTR[d]	This work
	1.4[a]	5.2[a]	5.2 ± 0.5	1.0 ± 0.1	V30M TTR[d]	
	3.2[a]	6.7[a]	4.5 ± 0.5	1.0 ± 0.2	T119M TTR[d]	
1,5-AmNS	–	–	64 ± 18	1.3 ± 0.4	wt TTR[d]	
	–	–	86 ± 25	1.3 ± 0.4	V30M TTR[d]	
	–	–	93 ± 43	1.3 ± 0.6	T119M TRT	

[a] Fitting error are equal or slightly larger than their respective K_d.
[b] 1.7–7.3 μM TTR, 50 mM phosphate, 100 mM NaCl, 1 mM EDTA, pH 7.4, 25 °C; Method: equilibrium dialysis.
[c] 4.8 μM TTR, 50 mM Tris, 100 mM NaCl, 1 mM EDTA, pH 5.6, 7.4 and 8.6, 25 °C; Method: direct fluorescence titration.
[d] 100 nM TTR, 20 mM phosphate pH 7.4, 100 mM KCl, 25 °C; Method: direct fluorescence titration.

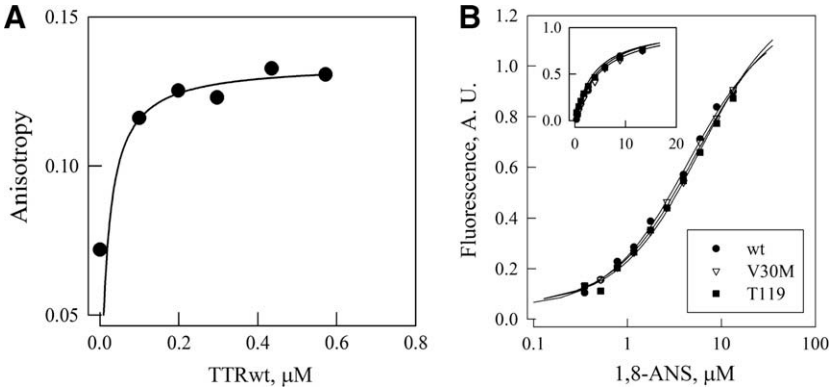

Figure 2. TTR interaction with 1,8-ANS. (A) Isothermal binding of 1,8-ANS to TTR measured by fluorescence anisotropy. 1,8-ANS (10 μM) was incubated with the indicated concentration of wtTTR and the fluorescence emission was measured and anisotropy calculated as indicated in Material and Methods; no corrections were performed for changes in fluorescence, and thus as most contribution in emission rises from the TTR-bound 1,8-ANS, an apparent asymptotic value is achieved much before all 1,8-ANS becomes complexed to the protein as shown if Figure 2B. (B) 1,8-ANS binding to TTR variants (wt, T119M and V30M). TTR (100 nM) was incubated with 1,8-ANS at indicated concentrations for at least 30 min and the fluorescence emission was measured. Ex 360 nm, Em 475 nm. All experiments were performed in 20 mM sodium phosphate buffer, 100 mM KCl, pH 7.4, at 25 °C. Details in Section 5.

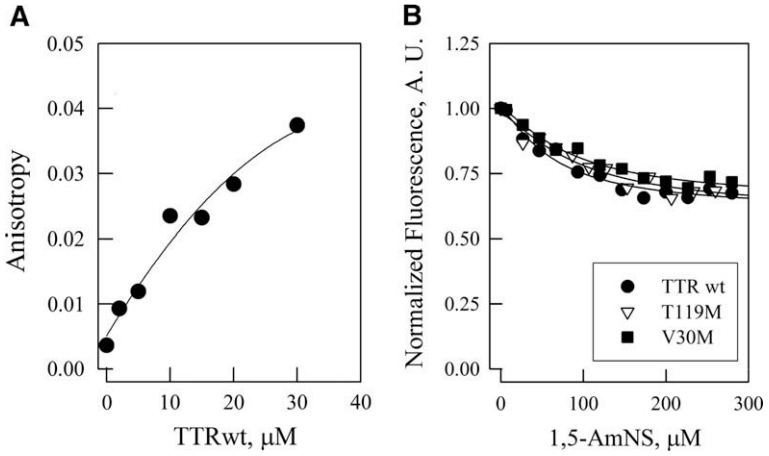

Figure 3. TTR interaction with 1,5-AmNS. (A) Isothermal binding of 1,5-AmNS to TTR measured by fluorescence anisotropy. 1,5-AmNS (100 nM) was incubated with the indicated concentration of wtTTR, the fluorescence emission was measured and anisotropy calculated as indicated in Section 5. No corrections were performed for changes in fluorescence. (B) 1,5-AmNS binding to TTR variants (wt, T119M and V30M) measured by quenching of TTR intrinsic fluorescence. TTR (100 nM) was incubated with 1,5-AmNS at indicated concentrations for at least 30 min and the fluorescence emission was measured. Ex was equal to 280 nm, and Em to 300–420 nm. All experiments were performed in 20 mM sodium phosphate buffer, 100 mM KCl, pH 7.4, at 25 °C. More details are given in Section 5.

ligands (data not shown). After final refinement and water search, no other large and continuous electron density was found, ruling out the possibility of ligand binding to other TTR regions in the crystal.

Table 2
Summary of X-ray crystallographic data collection and refinement

TTR:ligand	—	1,8-ANS	1,5-AmNS	Diclofenac
Space group	$P2_12_12$	$P2_12_12$	$P2_12_12$	$P2_12_12$
Resolution range (Å)	17.9–1.60 (1.64–1.60)	38.4–1.87 (1.92–1.87)	26.2–1.87 (1.92–1.87)	35.7–2.09 (2.14–2.09)
Unit cell dimension (Å)	43.2, 86.1, 63.8	43.3, 86.5, 63.5	43.0, 85.6, 63.8	43.1, 85.5, 63.6
Monomers/asymmetric unit	2	2	2	2
Multiplicity	6.9 (6.7)	7.2 (6.9)	4.1 (4.0)	4.1 (4.0)
Completeness (%)	99.9 (99.9)	93.5 (93.5)	96.8 (96.8)	94.7 (94.7)
$I/\sigma(I)$	25.7 (4.8)	30.6 (10.5)	16.4 (2.6)	14.2 (4.1)
R_{merge} (%)	4.6 (39.8)	4.3 (18.4)	5.9 (46)	7.4 (33.1)
Refinement				
No. of reflections used in refinement	30,418 (2153)	18,303 (1238)	18,738 (1282)	12,938 (946)
No. of reflections used for R_{free}	1624 (120)	994 (67)	1017 (56)	696 (57)
R_{work}/R_{free} (%)	19.1 (32.8)/21.8 (31.4)	20.0 (22.0)/24.5 (27.0)	19.1 (29.8)/23.9 (32.8)	20.9 (24.4)/24.8 (34.2)
B-factor (Å^2)				
Protein	19.4	15.1	19.7	24.4
Ligand	—	17.8	34.0	50.3
Water	33.9	29.9	32.2	32.7
Precision of atomic location[a] (Å)	0.17	0.18	0.21	0.25
Ramachandran outliers	0/230	0/230	0/230	0/230
RMSD bond length (Å)	0.007	0.007	0.019	0.006
RMSD bond angles (°)	1.06	1.08	1.66	1.12

Number in parentheses indicate the highest resolution shell.
R_{free} calculated for ⩾5% randomly chosen reflections that were excluded from the refinements.
[a] Upper limit of error in atomic coordinates as obtained by the method of Luzzati (1952).

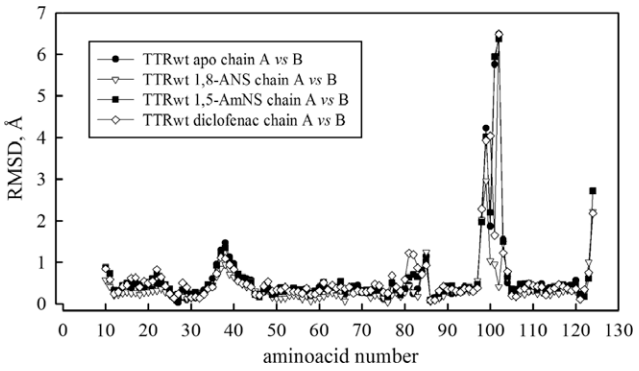

Figure 4. Comparative analysis between monomers of apo TTR. Monomer A and B of wtTTR were superposed (with program LSQKAB, from the CCP4 suite) and the RMSD of Cα are displayed for the apo form (closed circles) and in complex with 1,8-ANS (open triangles), 1,5-AmNS (closed squares) and diclofenac (opened diamonds).

Diclofenac is a well-known non-steroidal anti-inflammatory drug (NSAD) that can bind to wtTTR with high affinity with anti-aggregating activity.[11] A crystal structure of wtTTR:diclofenac complex has already been described;[11] (PDB entry 1DVX). For a more detailed comparative analysis of the effects of anilinonaphthalenes compounds binding to wtTTR, we used diclofenac as a reference compound, solving its crystal structure in complex with wtTTR in the same crystallization conditions used for 1,8-ANS and 1,5-AmNS. This approach permits a better and unbiased comparison, avoiding mis-interpretation of the data due to changes in experimental protocols such as pH, temperature, salt, and other co-solutes.[32]

The overall structures of wtTTR in complex with these three ligands were kept unchanged upon complexation, as evidenced by the low (<0.5 Å) deviation in Cα distances between the aligned monomers (Fig. 5). Complexation with the ligands also did not affect extensively protein temperature factors (B-factors), which fluctuated randomly when compared to the apo form (Fig. 6A, 7A and 8A). The absence of systematic changes in B-factors is suggestive of ligand binding to wtTTR with no major changes in the protein structure and dynamics.

2.4. Local effects of ligand binding

A large series of ligands have been studied for their interaction with TTR, and their inhibitory aggregating activity, binding affinity, complex crystal structure among other properties have been characterized.

Most of the ligands display negative cooperativity in the interaction with wtTTR, usually with the K_d in the nM or μM range. Another recurrent feature of ligand binding to TTR is its ability of interactions with all these compounds with minor or no effect in protein global and local protein structure, regardless of crystallization conditions, space group and ligand orientation. Very few ligands are able to induce changes at the level of amino acid residues side chain rotamers involved in direct ligand recognition, such as Ser117 and Thr119. Here we present the crystal structures of TTR in complex with three ligands, and discuss the molecular basis of interaction and implications for the improvement of compounds targeting inhibition of TTR aggregation.

2.4.1. wtTTR:diclofenac

The present diclofenac-bound wtTTR structure (PDB entry 3CFQ) displays large similarity with the previous reported structure (PDB entry 1DVX ;[11]), with an overall RMSD of 0.29 Å, which is negligible at the precision of atomic location of the present structures (Table 1). Diclofenac binding to both sites occurs with minimal side chains rearrangements compared to the apo wtTTR (PDB entry 3CFM; Fig. 6B and C).

Comparison between the present wtTTR:diclofenac complex (PDB entry 3CFQ) and previous reported structure (PDB entry 1DVX) shows considerable changes within the HBS and in the orientation of the diclofenac molecule in one of the binding sites (Fig. 6D).

In the previous structure (PDB entry 1DVX), the diclofenac molecules where shown to bind in similar fashion in both the AC and BD sites.[11] In this complex, the Ser117 and Thr119 from both channels flip their hydroxyl groups toward the thyroxine binding site

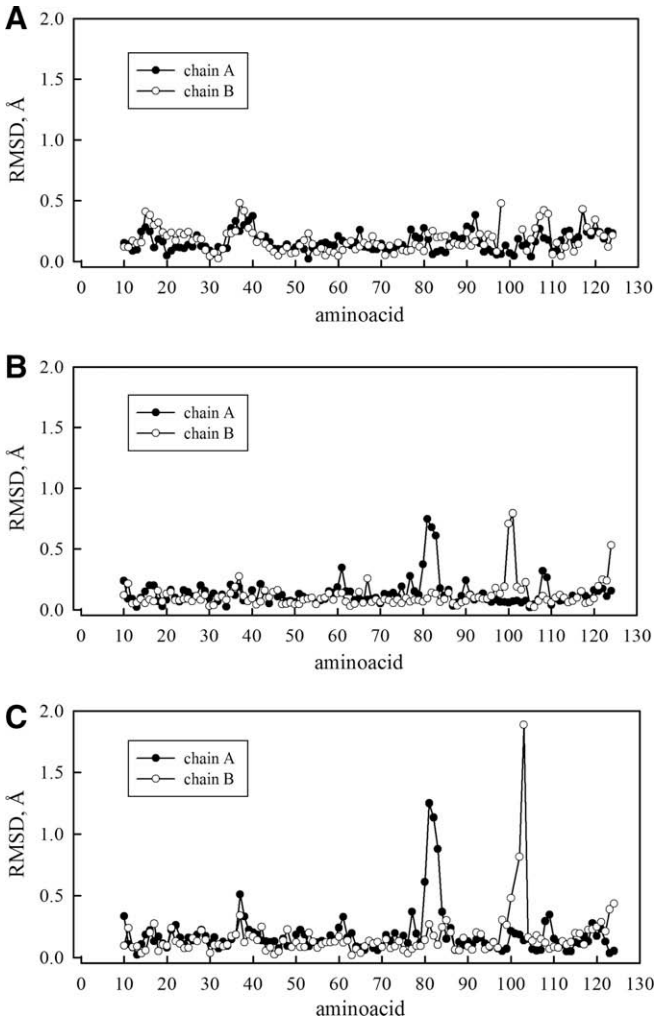

Figure 5. Comparative analysis between apo and ligand-complexed wtTTR structures. Each TTR complex was superposed (with program LSQKAB from the CCP4 suite) with the apo TTR (3CFM.pdb) and the RMSDs of Cα are displayed for (A) 1,8 ANS (3CFN.pdb), (B) 1,5-AmNS (3CFT) and (C) diclofenac (3CFQ.pdb).

allowing the formation of direct hydrogen bonding with the carboxylate group of diclofenac. Moreover, the alternate side chain conformation adopted by Thr119 also allows van der Waals interaction between its Cγ atom and the chlorine atoms from diclofenac, in addition to van der Waals interactions provided by amino acid side chains from others adjacent amino acids. On the contrary, our wtTTR:diclofenac structure shows only the Thr119 from the AC site in two alternate conformations, which in conjunction with Ser117 are involved in hydrogen bonding interaction with the acetate group of diclofenac (Fig. 6E).

The diclofenac molecules in the present structure (PDB entry 3CFQ) are orientated in dissimilar mode. In the BD channel, the diclofenac molecule is in good superposition with the diclofenac molecule from the previous structure (PDB entry 1DVX; Fig. 6D). The diclofenac molecule from BD site in wtTTR:diclofenac structure described here (PDB entry 3CFQ) is oriented with its two chlorine substituents inserted into the outer halogen binding pocket delimited by the Lys15, Leu17, Ala108 and Leu110 amino acid side chains.

In the opposite mode, the diclofenac molecule in the AC channel displays the dichlorophenyl ring rotated by approximately 90° (Fig. 6D), with the chlorine atoms inserted in the pocket delimited by side chains of Ala108, Thr119 and Leu17. Such a large difference in orientation of the second diclofenac molecule inside the HBS suggests that TTR has an inherent ability for ligand binding with low specificity, and thus motivates the search for compounds with a higher specificity to TTR.

2.4.2. wtTTR:1,5-AmNS

The crystal structure of wtTTR in complex with1,5-AmNS shows the ligand oriented in the middle of the HBS, in similar orientation for both sites (AC and BD; Fig. 7B and C). 1,5-AmNS binding to wtTTR is mediated by electrostatic interaction between its sulfonate group and the amine moiety of Lys15 side-chain (Fig. 7D). Additionally, the 1,5-AmNS amino group forms a hydrogen bond with a water molecule coordinated by the side-chain hydroxyl group from the amino acid residues of the innermost halogen binding pocket, Ser117 and Thr119 (Fig. 7D). Hydrophobic partition drives 1,5-AmNS binding to TTR, which leads to the stacking of its naphthalene moiety in the central part of the channel and in close proximity (3.4–3.8 Å) to side chains of amino acid residues Leu17, Ala108 and Leu110 (Fig. 7C). These data are consistent with the observed weak binding affinity of 1,5-AmNS to TTR (Table 1). In line with the above depicted wtTTR:diclofenac interaction, these data indicate that ligand binding to TTR with moderate affinity (micromolar range) can be supported by a few polar contacts and a few van der Waals interactions.

2.4.3. wtTTR:1,8-ANS

1,8-ANS binding to wtTTR occurs at a cost of changes in the HBS and adjacent amino acids (Fig. 8). Both sites (AC and BD) shows the 1,8-ANS with high occupancy and electron density map, revealing the same orientation and binding mode. In all TTR crystal structures available to date both in the apo form and complexed to ligands, the Lys15 and Leu17 side chains are in close proximity. However, these side chains move apart, giving place to a new cleft where 1,8-ANS stacks (Fig. 8C and D). Nonpolar contacts between the naphthalene ring of 1,8-ANS and the aliphatic part of the Lys15 and Leu17 side chains are formed, and the sulfonate moiety of 1,8-ANS is tightly bound by an electrostatic contact with the amine from Lys15 (Fig. 8D). Additionally, Thr119 rotates about 90° compared to the apo form (carbons in gray), establishing one water-mediated hydrogen bonding with the 1,8-ANS sulfonate moiety (Fig. 8D). In the apo form, the Thr119 hydroxyl group performs one water-mediated interaction with the hydroxyl from the Ser117 side chain (Fig. 8D; water molecules are represented by red spheres), which is disrupted upon 1,8-ANS binding releasing this water molecule, as suggested by its absence in the wtTTR:1,8-ANS crystal structure. Similar to the 1,5-AmNS and diclofenac, the hydrophobic aniline group of 1,8-ANS faces the middle of the low-polarity HBS (Fig. 8C). The novel cavity opened between Lys15 and Leu17 is a wide region able to perform extensive van der Waals contact with the ligand. Moreover, the opposing sulfonate moiety from 1,8-ANS is located in close proximity to the related electrophilic amine from Lys15′ (Fig. 8D), providing additional interactions with TTR.

2.5. Ligand activity against TTR fibril formation

We evaluated the activity of the ligands as inhibitors of TTR fibril formation using the standard fibril formation assay[10,11] (Table 3). wtTTR was allowed to equilibrate with ligands at pH 7.5 for 30 min and then challenged for fibril formation by lowering the pH to 4.6 for 72 h. Diclofenac and 1,8-ANS at 20 μM, a concentration sufficient to reach HBS saturation (Fig. 2B), led to a decrease in wtTTR aggregation in a similar extent. On the contrary, 1,5-AmNS did not show any significant fibril formation inhibition activity in the conditions assayed, which might be attributed of its limited affinity to TTR (Fig. 3B). Altogether, these data suggest

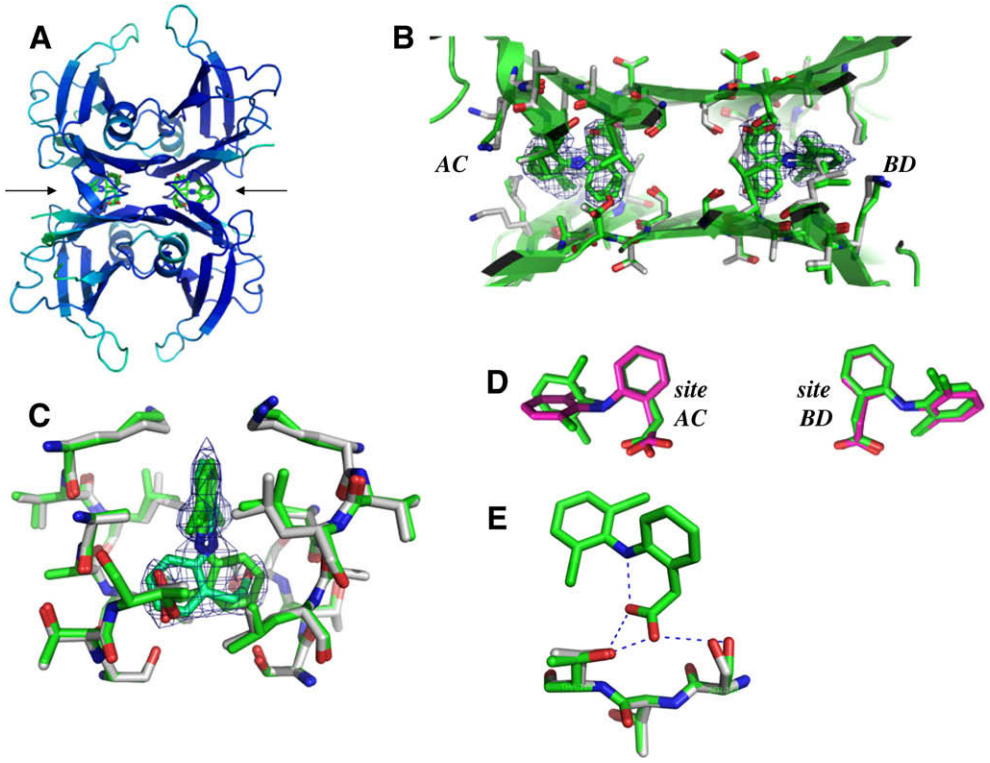

Figure 6. Comparative analysis of diclofenac interaction with TTR. (A) General view of tetrameric structure of wtTTR:diclofenac complex colored by B-factors, showing two diclofenac molecules inside the two binding sites (indicated by arrows). (B–D) Apo wtTTR (carbon atoms shown in gray) is compared to wtTTR in complex with diclofenac (green colored carbon atoms). (B) Detailed view of the HBS, (C) diclofenac interaction with wtTTR in the AC site (comprising aminoacids Lys15, Val16, Leu17, Ala108, Ala109, Leu110, Ser117, Thr118 and Thr119), depicting the contacting amino acid residues and showing the ligand electron density map, (D) superposition of diclofenac molecules from the present structure (carbon atoms colored in green; PDB entry 3CFQ) and the previously reported structure (carbon atoms given in magenta; PDB entry 1DVX;[11]) obtained after alignment of both TTR structures. (E) Detail of diclofenac interaction with wtTTR, depicting hydrogen bonding between carboxylic group from diclofenac and hydroxyl groups from Thr119 and Ser117. Dotted lines represent contacts with distances between 2.5 and 3.4 Å. Grids correspond to the OMIT $2F_O - F_C$ map contoured at 1σ.

novel features of the channel, revealing an extension of the thyroxine binding site that might be taken into account in future design of tight and selective compounds targeting TTR.

3. Discussion

Individuals with transthyretin related diseases currently do not have available an efficient therapy for their health conditions. Liver transplantation[33–35] is the only available choice, which is invasive and unfortunately is not efficient for all pathologies. Therefore, there is an immediate demand for both efficient and safe therapies. Genetic therapy with the variant T119M[30,36–38] and traditional small molecule based therapy, aiming the kinetic stabilization of the tetramer, are two approaches that are currently subjected to intense scientific research for ameliorating transthyretin amyloid disease.

The design of ligands targeting TTR is a difficult task. Treatment would demand long-term, life-long needs characteristic of the TTR-related diseases. Moreover, TTR is an abundant serum protein, and therefore small molecule compounds should be administered at high doses. In addition, TTR display low specificity for ligand binding, allowing the accommodation of a large diversity of compounds from several pharmacological classes in different orientations. Altogether, all these properties represent a challenge in the design of a new molecular entity targeting TTR both selectively and with high affinity. In this context, structural and molecular characterization of unique feature related to TTR would assist in this intricate task.

This work provides new insights for ligand design targeting TTR. We report a functional and structural analysis of TTR interaction with small compounds, revealing novel dynamic features of the HBS, which might be useful for the structure-based design of specific ligands directed to TTR binding. Here we demonstrate that 1,5-AmNS binding to TTR is supported by strong hydrogen bonding between Lys15 and the sulfonate moiety, and through a water-mediated hydrogen bonding between the amino group and Thr119 and Ser117. Hydrophobic interaction between the naphthalene ring also play an important role in partition. Despite of these interactions, 1,5-AmNS does not seem to be effective as a promising lead compound due to its lack of activity at moderate concentrations.

However, the binding of 1,8-ANS is due to the novel binding motif unraveled in TTR (Fig. 8). This binding mechanism is not present in any TTR structure described so far, as judged by a survey of the deposited structures in the PDB to date. Opposite to the loose binding of 1,5-AmNS, our crystallographic data revealed a tight binding site for 1,8-ANS, with close-fitting to this novel, well-delimited binding environment. Interestingly, 1,8-ANS binding revealed a novel feature of TTR recognition: 1,8-ANS inserts itself between Lys15 and Leu17, strongly anchored by two hydrogen bonds of 1,8-ANS sulfonate with Lys15′ and Thr119′ from the opposite monomer which forms the HBS. This new facet of TTR: ligand recognition, which allows the accommodation of a ligand in the HBS through novel, strong and well defined interactions, demonstrate that TTR has a dynamically articulated channel rooted within a relatively rigid molecular structure. Moreover, 1,8-ANS complexation to TTR results in considerable stabilization of the protein against fibril formation, which provides additional support for this binding mode as a candidate for optimization of compounds targeting TTR HBS.

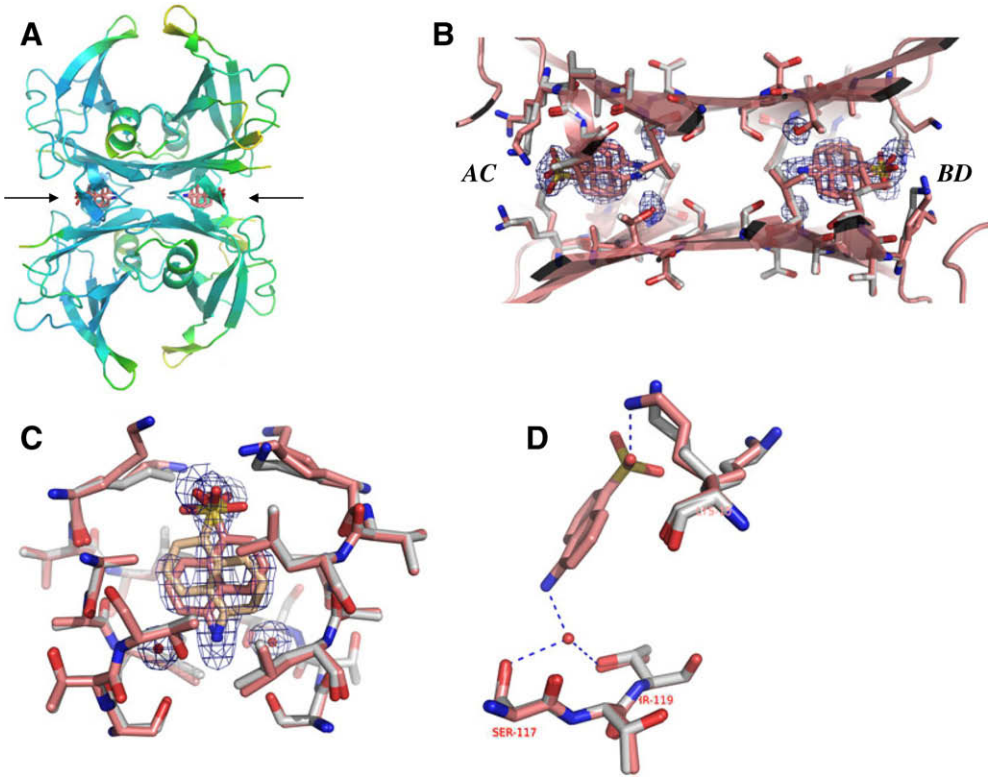

Figure 7. 1,5-AmNS interaction with TTR. (A) Tetrameric structure of wtTTR:1,5-AmNS complex colored by the B-factors, showing the two 1,5-AmNS molecules inside the two binding sites of the HBS (indicated by arrows). (B–D) Apo wtTTR (carbon atoms painted in gray) is compared to wtTTR in complex with 1,5-AmNS (pink colored carbon atoms), with a structural water molecule coordinated by Ser117 and Thr119. (B) A view of the HBS, (C) 1,5-AmNS interaction with wtTTR in the AC site (comprising aminoacids Lys15, Val16, Leu17, Ala108, Ala109, Leu110, Ser117, Thr118 and Thr119), depicting the contacting amino acid residues and the ligand electron density map, (D) wtTTR interactions with 1,5-AmNS are mediated by Lys15, Ser117 and Thr119. Dotted lines represent contacts with distances between 2.5 and 3.4 Å. Grids correspond to the OMIT $2F_O - F_C$ map contoured at 1σ.

Diclofenac binding to TTR occurs with very high affinity.[39] However, ligand docking into the channel is not as well defined as would be expected by the measured affinity, with K_d of 60 and 1200 nM for the first and second binding events.[39] Instead, we have shown a considerable difference in orientation for a same protein:ligand complex, that is, TTR:diclofenac (PDB entries 1DVX and 3CFQ; Fig. 8D), solved from two different crystallization conditions. Such difference might have origin in crystal packing effects over TTR conformation. However, we believe that TTR inherent structural features in the HBS are more likely to be the main reasons for the observed difference in orientation. In addition, we reported in this work the crystal structure of TTR in complex with the small ligand 1,5-AmNS, whose location in TTR channel was well defined despite their limited interactions. This is additional evidence that ligand binding by TTR can be driven more extensively due to hydrophobic partition, with minor specific and direct protein–ligand interactions.

The observed differences in A and B chains (Fig. 4), also observed in most TTR structures reported to date, are not changed upon interaction with the three ligand shown here. On the contrary, we observed alternative conformations for a few amino acid side chains, such as Lys15 in site AC, right at the entrance of the channel, which might reflect an explanation for the known cooperativity in ligand binding by TTR. Diclofenac binding to TTR as reveled by our structure (PDB entry 3CFQ) occurs in two dissimilar fashions, with the dichlorophenyl ring rotating on almost 90° when compared sites AC and BD. This indicates a large difference in ligand accommodation within the sites, which seems to be a structural manifestation of the negative cooperative in diclofenac binding to TTR, leading to K_d for first and second sites in the nanomolar and micromolar concentration range. On the other hand, we observed no detectable cooperative contribution in TTR interaction with 1,5-AmNS and 1,8-ANS, at the same time as no differences in orientation of these ligands were found in their crystal structures. We believe that, complimentary to the inherent structural arrangement in TTR structure, minor structural differences in ligand interaction might help explain the basis for the cooperative behavior of ligand binding by TTR, deserving a more extensive survey of the scientific literature accumulated to date.

We argue that this novel ligand binding motif in the HBS revealed by 1,8-ANS might be useful in the design of selective compounds targeting TTR, since it presumably defines a novel pharmacophoric pattern of TTR binding. This notion is corroborated by 1,8-ANS activity against TTR aggregation and fibril formation. Although 1,8-ANS metabolism has been subjected to investigation,[40–42] we do not advocate for the use of 1,8-ANS as a direct therapeutic molecule. Instead, we believe that the new dynamic and structural features revealed by the 1,8-ANS binding could be taken into account in lead optimization targeting TTR. 1,8-ANS and its analogues would, thus, be an template for molecular hybridization and functionalization of compounds designed for better interaction through the HBS aiming the enhancement of ligand affinity and overall selectivity for TTR.

4. Conclusion

The similar K_d and Hill's cooperativity in 1,8-ANS and 1,5-AmNS binding with both wt, V30M and T119M variants suggest a similar structural and thermodynamic binding mechanism, and indicate that features revealed by the crystal structures of the present com-

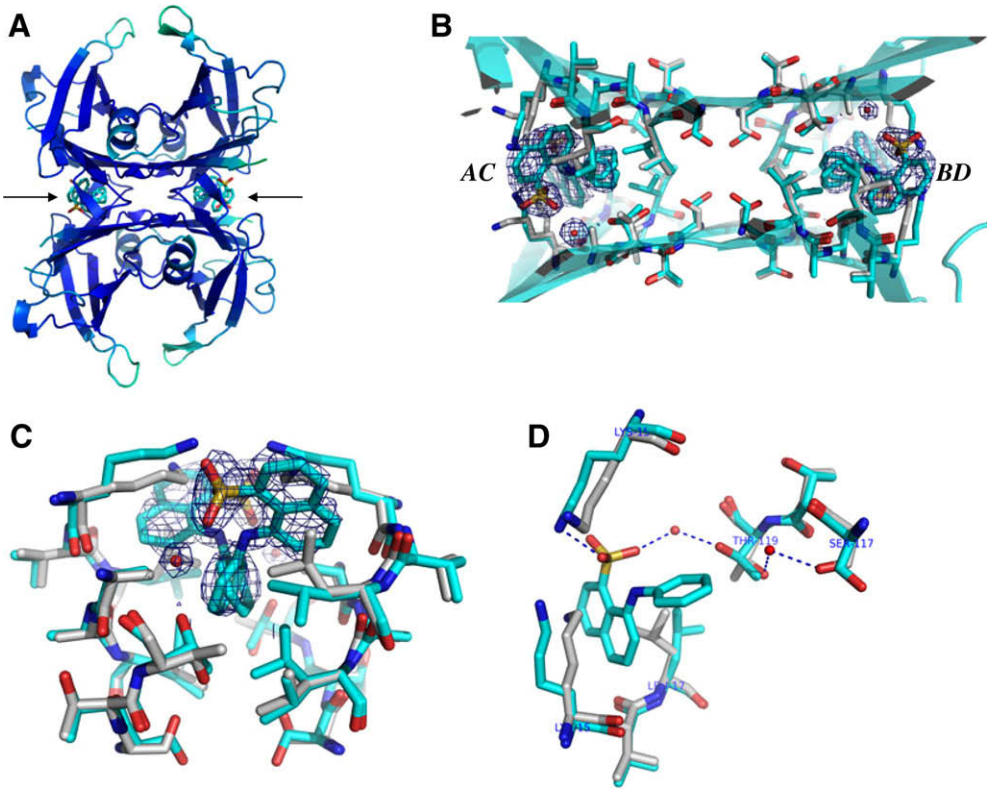

Figure 8. 1,8-ANS interaction with TTR. (A) Tetrameric structure of wtTTR:1,8-ANS complex colored by B-factors, showing two 1,8-ANS molecules inside the two binding sites of the HBS (indicated by arrows). (B–D) Apo wtTTR (carbon in gray) is compared to wtTTR in complex with 1,8-ANS (cyan colored carbons). (B) View of the HBS, (C) 1,8-ANS interactions with wtTTR in the AC site (comprising aminoacids Lys15, Val16, Leu17, Ala108, Ala109, Leu110, Ser117, Thr118 and Thr119), depicting the contacting aminoacids and the ligand electron density map, (D) Detailed view of wtTTR interaction with 1,8-ANS. The sulfonate moiety of 1,8-ANS performs a direct contact with the amine group of Lys15 side chain and a water-mediated hydrogen bonding with hydroxyl group of Thr119. Observe the Lys15 and Leu17 from apo form (carbon in grey) moving outward (carbons in cyan). This creates a cavity into which the naphthyl ring of 1,8-ANS is stacked. Dotted lines represent contacts with distances between 2.5 and 3.4 Å. Grids correspond to the OMIT $2F_O - F_C$ map contoured at 1σ.

Table 3
Ligand inhibition of wtTTR fibril formation

Compound	% Fibril
Diclofenac	33
1,8-ANS	44
1,5-AmNS	100

The protective role of tested compounds against wtTTR dissociation and fibril formation was evaluated, using 3.5 μM wtTTR and 20 μM compounds, as described in Section 5.
The error in these assays are ±5% or less.

plexes with wtTTR would be extensive to other TTR variants. Our work, in conjunction with previous studies, demonstrates that drug design targeting TTR should take into account the structural restrictions of this novel ligand binding motif in the HBS as revealed by 1,8-ANS and its inhibitory activity against TTR fibril formation. Rational lead-compound designed to bind to TTR would take advantage of the extension of the thyroxine binding pocket beyond the currently known limits.

5. Experimental

5.1. Chemicals

All reagents were of analytical grade. 1,8-ANS (Compound **1**; Fig. 1), ammonium salt, was obtained from Sigma–Aldrich; 1,5-AmNS, free acid, was obtained from Riedel-de-Haënand; diclofenac, potassium salt, was obtained from Galena (São Paulo, Brazil). Distilled water was deionized to less then 1.0 μS and filtered through a 0.22 μm pore-size membrane in a water purification system prior to use.

5.2. TTR expression and purification

TTR plasmids were kindly provided by Dr. Jeffery W. Kelly (The Scripps Institute, San Diego, California, USA). Recombinant human transthyretin, wild-type (wtTTR) and the variants V30 M and T119 M, were purified after recombinant expression in *Escherichia coli* as previously described.[27,43] Protein concentration was determinate using the protein extinction coefficient ε of 77,600 $M^{-1}cm^{-1}$ at 280 nm.

5.3. Fluorescence anisotropy

All fluorescence measurements were performed in a Jasco FP-6300 spectrofluorimeter (Jasco, USA), with appropriate corrections for blanks and controls. Anisotropy measurements were assembled in 'L' geometry, using excitation and emission wavelength 360 nm/500 nm for 1,8-ANS and 340 nm/500 for 1,5-AmNS. Anisotropy values R were calculated according to the equation:[44]

$$R = [I_{VV} - (G * I_{VH})]/[I_{VV} + (2^{*}G^{*}I_{VH})] \quad (1)$$

where I refers to the measured fluorescence intensity, and indexes V (vertical) and H (horizontal) are the position of the polarizes at excitation (first index) and emission (second index), and G is a correction factor which takes into account the differences in sensitivity in the two directions I_{VV} and I_{VH} according to:

$$G = I_{HV}/I_{HH} \quad (2)$$

For each sample, anisotropy was measured until absolute errors were less than 0.005. 1,8-ANS and 1,5-AmNS interaction with wtTTR, V30 M and T119 M is fast, reaching equilibrium in a few seconds, without further changes with prolonged equilibration (data not show).

5.4. Titrimetric assay of 1,8-ANS:TTR interaction

Isothermal titrimetric assay of 1,8-ANS binding to TTR was performed in 20 mM sodium phosphate, 100 mM KCl, pH 7.4 at 22 °C. Two methods with equivalent results were used to measure ANS binding to TTR, as follow:

Method 1. Sequential addition: A concentrated solution ANS was sequentially added to a fixed amount of TTR, homogenized and equilibrated for 2 min prior to fluorescence measurements. In all cases maximal dilution was less than 5%. Changes in fluorescence intensity and ANS and TTR concentrations were corrected for dilution. Fluorescence measurements were performed in a Jasco FP6300 spectrofluorimeter (Jasco Inc., Japan), assembled in 'L' geometry. Excitation was set to 360 nm and emission was scanned between 400 and 600 nm. All experiments were performed at least three times and presented exactly similar behavior.

Method II. Serial dilution: Varying amounts of ANS was serially diluted and added of a fixed amount of TTR, homogenized and equilibrated for 30 min prior to fluorescence measurements. Changes in fluorescence intensity were properly corrected. Fluorescence measurements were performed in a Spectramax multiwell plate reader (Perkin Elmer). Excitation was set to 360 nm and emission was accumulated at 475 nm.

5.5. Titrimetric assay of 1,5-AmNS:TTR interaction

Isothermal titrimetric assay of 1,5-AmNS binding to TTR was performed in 20 mM sodium phosphate, 100 mM KCl, pH 7.4 at 22 °C, by fluorescence-resonance energy transfer (FRET). A concentrated solution AmNS was sequentially added to a fixed amount of TTR, homogenized and equilibrated for 2 min prior to intrinsic protein fluorescence measurements. In all cases maximal dilution was less than 5%. Changes in intrinsic protein fluorescence intensity and 1,5-AmNS and TTR concentrations were properly corrected for dilution and inner filter effect using L-tryptophan as fluorescent probe. Fluorescence measurements were performed in a Jasco FP6300 spectrofluorimeter (Jasco Inc, Japan), assembled in 'L' geometry, with excitation set to 280 nm and emission scanned between 300 and 400 nm. All experiments were performed at least three times and presented exactly similar behavior.

5.6. Analysis of binding isotherms

We used a considerably high concentration (100 nM TTR) as compared to the dissociation constants. In this case, a 'tight binding' model[45–48] should apply, since the total amount of ligand significantly differ from free concentration, and thus the total amount of protein is taken into account. For ANS and AmNS binding to TTR, we considered the following two-state reversible equilibrium between these compounds (ligands, 'L') and TTR:

$$\mathrm{TTR} + 2\ \mathrm{L} \leftrightharpoons [\mathrm{TTR} : \mathrm{L}_2]$$

Thus, we define the dissociation constant K_d of the above reaction according to

$$K_d = (P * L^n)/\mathrm{PL}_2 \quad (3)$$

where P is the molar concentration of free tetrameric TTR, L is the molar concentration of free ligands, PL_2 is the molar concentration of complex formed between TTR and the ligands and 'n' accounts for both the number of sites, cooperativity and different quantum yield of TTR-bound compounds that may differ according to particular properties of each binding site.The complex is related to fluorescence intensity by:

$$\mathrm{PL}_2 = P_t * \alpha \quad (4)$$

where

$$\alpha = \text{fraction of TTR(or ANS)associated} = (\mathrm{Fobs} - A)/(B - A) \quad (5)$$

and Fobs is the observed fluorescence intensity, A and B are, respectively the lower and upper asymptotic limits for fluorescence values obtained by fitting the curves.

For an interactive binding model, it follows that

$$\mathrm{Fobs} = A + (B - A) * ((K_d^n + L_t^n + P_t) - ((K_d^n + L_t^n + P_t)^2 - 4^* L_t^n * P_t)^{0.5})/(2 * P_t) \quad (6)$$

where P_t, the total molar concentration of tetrameric TTR employed in the assay, corresponds to the sum of free (P) and bound (PL_2) TTR concentrations and L_t is the total ligand concentration. This apparent cooperative parameter 'n' may become equal to 1 in case two independent sites model do apply. However, it is not straightforward to extract the real contributions of fluorescence to fractional binding, since changes in it may reflect changes in quantum yield due to chemical environment induced by both allosteric components associated to conformational transition of TTR upon complexation as well as non-linearity of fluorescence intensity as a function of site occupation.For an independent binding model, equation comes from the sequential summation of two equivalent Eq. (6):

$$\mathrm{Fobs} = A + (B - A) * ((K_{d1} + L_t + P_t) - ((K_{d1} + L_t + P_t)^2 - 4 * L_t * P_t)^{0.5})/(2 * P_t) + (C - B) * ((K_{d2} + L_t + P_t) - ((K_{d2} + L_t + P_t)^2 - 4 * L_t * P_t)^{0.5})/(2 * P_t) \quad (7)$$

where K_{d1} and K_{d2} are the dissociation constants for the two ligand binding event, and A, B, and C are the fluorescence intensity corresponding to free species, one site occupation and second site occupation.Eqs. 6 and 7 were adjusted to data by non-linear least-squares regression using SigmaPlot (version 10.0, Jandel Scientific Co).

5.7. wtTTR crystallization, data diffraction and structure solution

TTR crystals in the apo form (without ligand) were obtained by the hanging drop vapor-diffusion method. Diffraction quality crystals of about $0.8 \times 0.8 \times 0.5\ \mathrm{mm}^3$ grew at 18 °C in 5 days from 2 μL drops containing 5 mg/mL TTR, 11% PEG 400, 50 mM Tris and 50 mM KCl, pH 7.4, equilibrated against 22% peg 400, 100 mM Tris and 100 mM KCl, pH 7.4. The TTR complexes with 1,8-ANS, 1,5-AmNS and diclofenac were prepared by soaking apo wtTTR crystals into mother liquor containing excess compounds for 1 h. X-ray diffraction data set were collected from N_2 stream flash-cooled crystals at 100 K, using Cu Kα radiation (1.5418 Å), generated by a Rigaku UltraX 18 rotating anode operated at 50 kV and 90 mA and equipped with Osmic confocal Max-Flux optics, and recorded on a MAR 345dtb image plate. The images were indexed and processed with Mosflm[49] and scaled with Scala.[50] The structure of apo wtTTR was solved by molecular replacement with MolRep[51] using an apo form (despite of a non-characterized large electron density blob in the HBS) of the human TTR as search model (PDB entry 1F41). Structure refinement was conducted with Refmac.[52] No additional gain in quality was observed by the use of either TLS[53] or imposition of non-crystallographic symmetry. Real space refinement was conducted by visual inspection of both the map and

model with Coot,[54] also used for the addition of water molecules. This same data processing, structure solution and refinement was used for the complexes with 1,8-ANS (PDB entry 3CFN), 1,5-AmNS (PDB entry 3CFT) and diclofenac (PDB entry 3CFQ), but using the apo wtTTR structure reported here (PDB entry 3CFM) as the search model. Average atomic locations are precise to better than 0.25 Å (Table 1;[55]). Structural validation of the model performed with PROCKECK[56] showed all main-chain dihedral angle in the allowed regions, with exception of the poorly defined amino acids in the FG loop (aminoacids 99–102) in the B chains of both free and ligand-bound structures. All residues were found in favorable Ramachandram regions. A detailed report of structures statistics can be found in Table 2. As a result of a twofold symmetry of the binding sites, each ligand molecule was refined at 0.5 of occupancy and they are partially superposed with its copy generated by the twofold symmetry. OMIT maps were generated with OMIT program[57] from CCP4 suite.[58] For color figures, oxygen atoms are shown in red, nitrogen in blue, sulfur in yellow, chlorine in green and hydrogen atoms are excluded. Important water molecules are represented as red spheres. All figures were generated with PyMol.[59]

5.8. Fibril formation assay

Inhibitory activity of compounds against wtTTR fibril formation was studied as described elsewhere.[10,11] In brief, 7.0 μM wtTTR was pre-incubated with varying concentrations of ligands (diclofenac, 1,8-ANS or 1,5-AmNS, from stock solution in water) in 10 mM sodium phosphate, 50 mM KCl, pH 7.5 in the presence of varying concentrations of. After 30 min incubation at 37 °C, samples were acidified to pH 4.6 with equal volume of 200 mM sodium acetate/100 mM KCl buffer, to provide 100 mM acetate, 50 mM KCl and 3.5 μM wtTTR final concentrations. Samples were them left at 37 °C for 72 h, vortexed and them evaluated for the extent of aggregation (fibril formation) by light scattering at 500 nm (for both excitation and emission, in a Jasco FP6300 spectrofluorimeter; Jasco Inc, USA) and with similar results by turbidimetry at 500 nm (UV-Mini-1240 spectrophotometer, Shimadzu Corp, Japan). Experiment was performed in triplicate, and errors were typically below 5%. Blank scattering was subtracted accordingly and data were normalized to the percentage of fibrils by taking aggregation in the absence of ligands as 100%.

Acknowledgments

We thank Dr. Astria Ferrão-Gonzales and Dr. Priscila S. Ferreira da Silva for assistance in protein purification, Mr. José Geraldo Catarino and Mr. José Augusto Lopes da Rocha from IFSC (USP) for excellent technical assistance and Leonardo C. Palmieri and Lucas Bleicher for suggestions. This work was supported by grants from Conselho Nacional de Desenvolvimento Científico e Tecnológico (CNPq), Millennium Institute for Structural Biology in Biomedicine and Biotechnology (CNPq Millennium Program), Fundação Carlos Chagas Filho de Amparo à Pesquisa do Estado do Rio de Janeiro (FAPERJ), Fundação de Amparo à Pesquisa do Estado de São Paulo (FAPESP) and Conselho de Aperfeiçoamento de Pessoal de Nível Superior (CAPES). PDB ID Codes: Atomic coordinates have been deposited in the RCSB Protein Data Bank (www.pdb.org) and are available under accession codes 3CFM (apo TTR), 3CFN (TTR in complex with 1,8-ANS), 3CFT (TTR in complex with 1,5-AmNS) and 3CFQ (TTR in complex with diclofenac).

References and notes

1. Blake, C. C.; Swan, I. D.; Rerat, C.; Berthou, J.; Laurent, A.; Rerat, B. *J. Mol. Biol.* **1971**, *61*, 217.
2. Blake, C. C.; Geisow, M. J.; Oatley, S. J.; Rerat, B.; Rerat, C. *J. Mol. Biol.* **1978**, *121*, 339.
3. Foss, T. R.; Wiseman, R. L.; Kelly, J. W. *Biochemistry* **2005**, *44*, 15525.
4. Cordeiro, Y.; Kraineva, J.; Suarez, M. C.; Tempesta, A. G.; Kelly, J. W.; Silva, J. L.; Winter, R.; Foguel, D. *Biophys. J.* **2006**, *91*, 957.
5. Westermark, P.; Sletten, K.; Johansson, B.; Cornwell, G. G., III *Proc. Natl. Acad. Sci. U.S.A.* **1990**, *87*, 2843.
6. Saraiva, M. J.; Costa, P. P.; Goodman, D. S. *J. Clin. Invest.* **1985**, *76*, 2171.
7. Jacobson, D. R.; Pastore, R. D.; Yaghoubian, R.; Kane, I.; Gallo, G.; Buck, F. S.; Buxbaum, J. N. *N. Eng. J. Med.* **1997**, *336*, 466.
8. Stangou, A. J.; Hawkins, P. N. *Curr. Opin. Neurol.* **2004**, *17*, 615.
9. Peterson, S. A.; Klabunde, T.; Lashuel, H. A.; Purkey, H.; Sacchettini, J. C.; Kelly, J. W. *Proc. Natl. Acad. Sci. U.S.A.* **1998**, *95*, 12956.
10. Wojtczak, A.; Cody, V.; Luft, J. R.; Pangborn, W. *Acta Crystallogr., Sect. D Biol. Crystallogr.* **1996**, *52*, 758.
11. Klabunde, T.; Petrassi, H. M.; Oza, V. B.; Raman, P.; Kelly, J. W.; Sacchettini, J. C. *Nat. Struct. Biol.* **2000**, *7*, 312.
12. Green, N. S.; Foss, T. R.; Kelly, J. W. *Proc. Natl. Acad. Sci. U.S.A.* **2005**, *102*, 14545.
13. Maia, F.; Almeida, M. R.; Gales, L.; Kijjoa, A.; Pinto, M. M.; Saraiva, M. J.; Damas, A. M. *Biochem. Pharmacol.* **2005**, *70*, 1861.
14. Johnson, S. M.; Connelly, S.; Wilson, I. A.; Kelly, J. W. *J. Med. Chem.* **2008**, *51*, 260.
15. Sekijima, Y.; Dendle, M. A.; Kelly, J. W. *Amyloid* **2006**, *13*, 236.
16. Jhoti, H. *Nat. Biotechnol.* **2005**, *23*, 184.
17. Hartshorn, M. J.; Murray, C. W.; Cleasby, A.; Frederickson, M.; Tickle, I. J.; Jhoti, H. *J. Med. Chem.* **2005**, *48*, 403.
18. Shuker, S. B.; Hajduk, P. J.; Meadows, R. P.; Fesik, S. W. *Science* **1996**, *274*, 1531.
19. Nienaber, V. L.; Richardson, P. L.; Klighofer, V.; Bouska, J. J.; Giranda, V. L.; Greer, J. *Nat. Biotechnol.* **2000**, *18*, 1105.
20. Babaoglu, K.; Shoichet, B. K. *Nat. Chem. Biol.* **2006**, *2*, 720.
21. Frederickson, M.; Callaghan, O.; Chessari, G.; Congreve, M.; Cowan, S. R.; Matthews, J. E.; McMenamin, R.; Smith, D. M.; Vinkovic, M.; Wallis, N. G. *J. Med. Chem.* **2008**, *51*, 183.
22. Hajduk, P. J. *J. Med. Chem.* **2006**, *49*, 6972.
23. Ferguson, R. N.; Edelhoch, H.; Saroff, H. A.; Robbins, J.; Cahnmann, H. J. *Biochemistry* **1975**, *14*, 282.
24. Nilsson, S. F.; Rask, L.; Peterson, P. A. *J. Biol. Chem.* **1975**, *250*, 8554.
25. Cheng, S. Y.; Pages, R. A.; Saroff, H. A.; Edelhoch, H.; Robbins, J. *Biochemistry* **1977**, *16*, 3707.
26. Raghu, P.; Reddy, G. B.; Sivakumar, B. *Arch. Biochem. Biophys.* **2002**, *400*, 43.
27. Ferrao-Gonzales, A. D.; Souto, S. O.; Silva, J. L.; Foguel, D. *Proc. Natl. Acad. Sci. U.S.A.* **2000**, *97*, 6445.
28. Lartigue, A.; Gruez, A.; Spinelli, S.; Riviere, S.; Brossut, R.; Tegoni, M.; Cambillau, C. *J. Biol. Chem.* **2003**, *278*, 30213.
29. Schonbrunn, E.; Eschenburg, S.; Luger, K.; Kabsch, W.; Amrhein, N. *Proc. Natl. Acad. Sci. U.S.A.* **2000**, *97*, 6345.
30. Coelho, T.; Carvalho, M.; Saraiva, M. J.; Alves, I.; Almeida, M. R.; Costa, P. P. *J. Rheumatol.* **1993**, *20*, 179.
31. Hornberg, A.; Eneqvist, T.; Olofsson, A.; Lundgren, E.; Sauer-Eriksson, A. E. *J. Mol. Biol.* **2000**, *302*, 649.
32. Furnham, N.; Blundell, T. L.; Depristo, M. A.; Terwilliger, T. C. *Nat. Struct. Mol. Biol.* **2006**, *13*, 184.
33. Tan, S. Y.; Pepys, M. B.; Hawkins, P. N. *Am. J. Kidney Dis.* **1995**, *26*, 267.
34. Holmgren, G.; Ericzon, B. G.; Groth, C. G.; Steen, L.; Suhr, O.; Andersen, O.; Wallin, B. G.; Seymour, A.; Richardson, S.; Hawkins, P. N. *Lancet* **1993**, *341*, 1113.
35. Suhr, O. B.; Ando, Y.; Holmgren, G.; Wikstrom, L.; Friman, S.; Herlenius, G.; Ericzon, B. G. *Transpl. Int.* **1998**, *11*, S160–S163.
36. Alves, I. L.; Divino, C. M.; Schussler, G. C.; Altland, K.; Almeida, M. R.; Palha, J. A.; Coelho, T.; Costa, P. P.; Saraiva, M. J. *J. Clin. Endocrinol. Metab.* **1993**, *77*, 484.
37. Hammarstrom, P.; Schneider, F.; Kelly, J. W. *Science* **2001**, *293*, 2459.
38. Palhano, F. L.; Leme, L. P.; Busnardo, R. G.; Foguel, D. *J. Biol. Chem.* **2009**, *284*, 1443.
39. Oza, V. B.; Smith, C.; Raman, P.; Koepf, E. K.; Lashuel, H. A.; Petrassi, H. M.; Chiang, K. P.; Powers, E. T.; Sachettinni, J.; Kelly, J. W. *J. Med. Chem.* **2002**, *45*, 321.
40. Chung, Y. B.; Miyauchi, S.; Sugiyama, Y.; Harashima, H.; Iga, T.; Hanano, M. *J. Hepatol.* **1990**, *11*, 240.
41. Chung, Y. B.; Miyauchi, S.; Sugiyama, Y.; Harashima, H.; Iga, T.; Hanano, M. *J. Pharmacokinet. Biopharm.* **1990**, *18*, 313.
42. Chung, Y. B.; Bae, W. T.; Han, K. *Arch. Pharm. Res.* **1998**, *21*, 677.
43. Lai, Z.; Colon, W.; Kelly, J. W. *Biochemistry* **1996**, *35*, 6470.
44. Lakowicz, J. R. *Principles of Fluorescence Spectroscopy*; Plenum Press: New York, NY, 1999.
45. Morrison, J. F. *Biochim. Biophys. Acta* **1969**, *185*, 269.
46. Bieth, J. G. *Methods Enzymol.* **1995**, *248*, 59.
47. Cantor, C. R.; Schimmel, P. R. *Biophysical Chemistry*; W.H. Freeman & Company: New York, 1980.
48. Lima, L. M. T. R.; Silva, J. L. *J. Biol. Chem.* **2004**, *279*, 47968.
49. Leslie, A. G. *Joint CCP4 + ESF-EAMCB Newsletter on Protein Crystallography*, **1992**.
50. Evans, P. R. *Joint CCP4 and ESF-EACBM Newsletter on Protein Crystallography* **1997**, *33*, 22.
51. Vagin, A.; Teplyakov, A. *J. Appl. Crystallogr.* **1997**, *30*, 1022.
52. Murshudov, G. N.; Vagin, A. A.; Dodson, E. J. *Acta Crystallogr., Sect. D Biol. Crystallogr.* **1997**, *53*, 240.

53. Winn, M. D.; Isupov, M. N.; Murshudov, G. N. *Acta Crystallogr., Sect. D Biol. Crystallogr.* **2001**, *57*, 122.
54. Emsley, P.; Cowtan, K. *Acta Crystallogr., Sect. D Biol. Crystallogr.* **2004**, *60*, 2126.
55. Luzzati, V. *Acta Crystallogr.* **1952**, *5*, 802.
56. Laskowski, R. A.; MacArthur, M. W.; Moss, D. S.; Thornton, J. M. *J. Appl. Crystallogr.* **1993**, *26*, 283.
57. Bhat, B. W. *J. Appl. Crystallogr.* **1988**, *21*, 279.
58. Collaborative Computational Project, N. 4. *Acta Crystallogr.* **1994**, 760.
59. DeLano, W. L. In DeLano Scientific LLC, San Carlos, CA, USA, 2002.